JOC The Journal of Organic Chemistry

Article

pubs.acs.org/joc

NMR Study of Hyperporphyrin Effects in the Protonations of Porphyrins with 4-Aminophenyl and 4-Pyridyl Meso Substituents

Chenyi Wang and Carl C. Wamser*

Department of Chemistry, Portland State University, Portland, Oregon 97207-0751, United States

Supporting Information

ABSTRACT: Titrations for a series of porphyrins bearing either 4-aminophenyl or 4-pyridyl meso substituents were performed using methanesulfonic acid in DMSO and followed by proton NMR. Special emphasis was placed on identifying the intermediate protonation stages that are described as hyperporphyrins, that is, where there exist strong charge-transfer interactions between the peripheral aminophenyl groups and the protonated porphyrin ring. In particular, evidence was gathered to support the significance of a novel resonance form involving charge transfer between two peripheral substituents, an aminophenyl group and a protonated pyridinium group. ^{1}H NMR and NOESY spectra provide evidence for the importance of such resonance effects in the triply protonated triamino/monopyridyl hyperporphyrin ($\mathbf{A_3PyPH_3}^{+3}$).

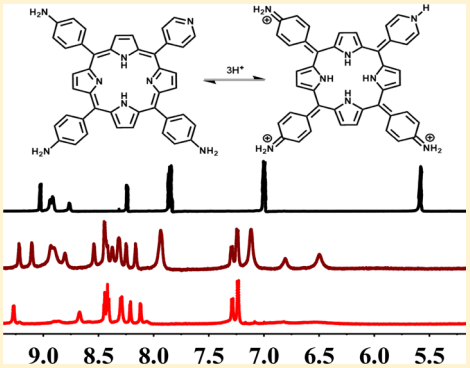

INTRODUCTION

The Gouterman four-orbital rule successfully describes the spectroscopy of regular porphyrins based on $\pi-\pi^*$ energy transitions between porphyrin molecular orbitals.[1] The term hyperporphyrin applies to those situations in which unusual spectroscopy is observed due to the involvement of additional orbitals leading to charge-transfer interactions.[2] These additional orbitals may come from a central metal in a metalloporphyrin[3−7] or from appropriate substituents, especially where such substituent effects are amplified by acid−base reactions.[2,8−13] The spectroscopy of a hyperporphyrin typically is marked by a strong and broad absorption at longer wavelengths than the regular Q-bands.[1] Because hyperporphyrins significantly extend the already remarkable spectroscopy of porphyrins, they are of substantial interest for potential optoelectronic applications.

Different categories of porphyrin spectra and structures have been defined to recognize the various types of interactions that can exist between peripheral substituents and the porphyrin ring and the concomitant effects of these interactions on the spectroscopy.[2,9] A and A′ describe regular porphyrins in which the porphyrin aromatic ring system is not significantly affected by metals or meso substituents. A and A′ exhibit D_{4h} and D_{2h} porphyrin core symmetry, respectively, and the Gouterman four-orbital rule applies well. A′-type spectra (D_{2h} symmetry, typically with 4 Q bands) are observed for free base porphyrins for which there are no significant interactions with any substituent or central metal ion. A-type spectra are observed for fully protonated porphyrins or metalloporphyrins (D_{4h} symmetry, typically with only two Q bands), again in the absence of any significant interactions with a substituent or central metal ion.

Hyperporphyrin spectra are observed when meso substituents, such as *p*-aminophenyl, provide strong electron donation to protonated porphyrins.[2,9,12,13] B-type describes a hyperporphyrin structure in which a single substituent strongly interacts with the porphyrin core such that a resonance form can be drawn with a single quinoid-type form (Figure 1). This type of hyperporphyrin is observed for diprotonated porphyrins bearing only one aminophenyl group or two amino groups in trans alignment.[9,12] The delocalization of the positive charge from the interior of the porphyrin ring to an aminophenyl substituent leads to a resonance form of the type illustrated below as hyperporphyrin B. In the structure illustrated, there are three different aminophenyls that could delocalize the charge in a B-type resonance.

C-type hyperporphyrin structures are characterized by two strong interactions with peripheral substituents leading to two quinoid structures in the resonance forms. C-type hyperporphyrin spectra are observed for porphyrins with two aminophenyl groups in cis alignment or with three or four aminophenyl substituents.[9,12] As with the B-type, the two central nitrogens still need to be protonated, but in this case delocalization can occur for both positive charges to two different aminophenyl substituents. A comparable resonance form simply cannot be drawn for trans aminophenyl substituents, and the hyperporphyrin spectroscopy is distinctly stronger for the cis isomer compared to the trans.[9,12] For the example shown below, there are two different cis orientations that can form a C-type resonance.

When an electron-withdrawing substituent such as pyridinium is included, as in this study, a novel type of hyperporphyrin resonance form has been proposed.[12] In this case additional charge-transfer interaction can include all four peripheral substituents in resonance with the porphyrin core, as illustrated

Received: March 27, 2015
Published: July 13, 2015

DOI: 10.1021/acs.joc.5b00690
J. Org. Chem. 2015, 80, 7351−7359

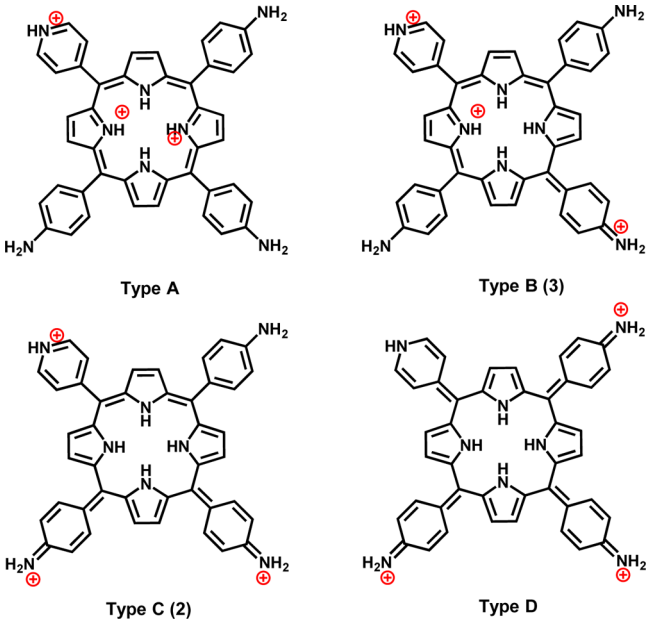

Figure 1. Different types of hyperporphyrin resonance forms for a representative protonated porphyrin, categorized based on the number of peripheral substituents interacting via resonance with the porphyrin core (0, 1, 2, or 4). Parenthetical numbers indicate the number of statistical possibilities for different substituents acting in the indicated manner.[12]

in structure D above. A major purpose of this study is to gain insight into the importance of such a resonance form in the overall structure and properties of the hyperporphyrin shown above. Because of the presence of a partially reduced pyridine ring and the suggestion that reduced pyridine forms may have electrocatalytic or photocatalytic activity,[14] there is significant interest in the structure and properties of such forms.

RESULTS

The NMR spectra of hyperporphyrins induced by protonation are typically very complex because of the multiple possible protonation states. Nevertheless, an early study of protonated porphyrins with *p*-(dimethylamino)phenyl substituents was successful in identifying hyperporphyrin NMR spectra.[11] The study showed that the addition of trifluoroacetic acid to the porphyrins caused the internal porphyrin N−H to be chemically shifted downfield, while the *β*-hydrogens of the pyrroles were found to move upfield during the formation of the hyperporphyrin form. These changes were attributed to diminished ring current effects, which could arise from geometric distortion of the porphyrin core.

The porphyrins in this study include three different potential sites for protonation—the porphyrin interior, the peripheral pyridyl groups, and the peripheral aminophenyl groups—and protonation states from neutral to +6. Spectrophotometric characterizations were successful in distinguishing the order of protonation and gave distinct spectra for most of the intermediate stages of protonation.[12] For these studies, we used a thin-layer cell to measure UV−vis spectra of the same solutions that were used for the NMR spectra, allowing us to identify the specific protonation state under study based on our earlier work.[12] The structures of the aminophenyl/pyridyl porphyrins are shown in Figure 2 with our standard abbreviations for each porphyrin.

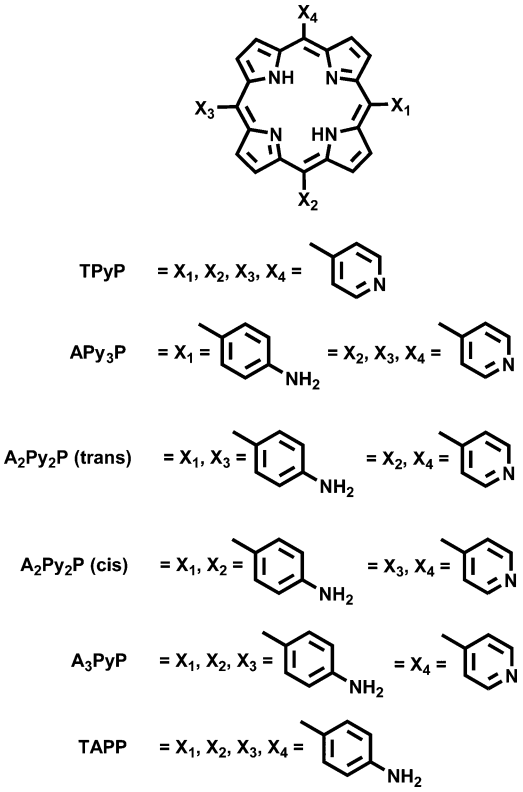

Figure 2. Structures and abbreviations for the aminophenyl/pyridyl porphyrins.

In identifying the various features of the NMR spectra, the different protons are distinguished by abbreviations for the corresponding positions: A = amino (NH_2), P = porphyrin (NH), Ph = phenyl (o or m), Py = pyridyl (2 or 3), and Pr = pyrrole (*β*) (Figure 3).

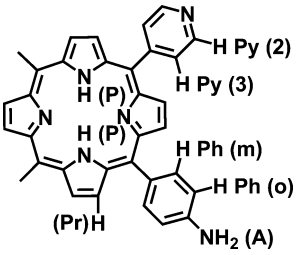

Figure 3. A general structure for aminophenyl/pyridyl porphyrins with notations used to designate individual hydrogens.

Before considering the complex NMR spectra of the various protonated forms of the mixed-substituent aminophenyl/pyridyl porphyrins, it is important to reference the NMR spectra of protonated tetra(4-pyridyl)porphyrin (**TPyP**) and tetra(4-aminophenyl)porphyrin (**TAPP**) as model compounds.

TPyP. All acid titrations were done using methanesulfonic acid (MSA) in DMSO. However, due to the inadequate solubility of free base **TPyP** in DMSO, a reference spectrum was taken in $CDCl_3$ (Figure 4). The free base **TPyP** spectrum in chloroform-D shows peaks at −2.93 (2H, s, P), 8.15−8.17 (8H, dd, Py-3), 9.06−9.07 (8H, dd, Py-2), 8.87 (8H, s, Pr). In order to solubilize **TPyP** in DMSO for further titrations, it was acidified beforehand with minimal MSA in DMSO. The initial protonation state was determined to be $\mathbf{TPyPH_4}^{+4}$ by the UV−vis spectrum and the

DOI: 10.1021/acs.joc.5b00690
J. Org. Chem. 2015, 80, 7351−7359

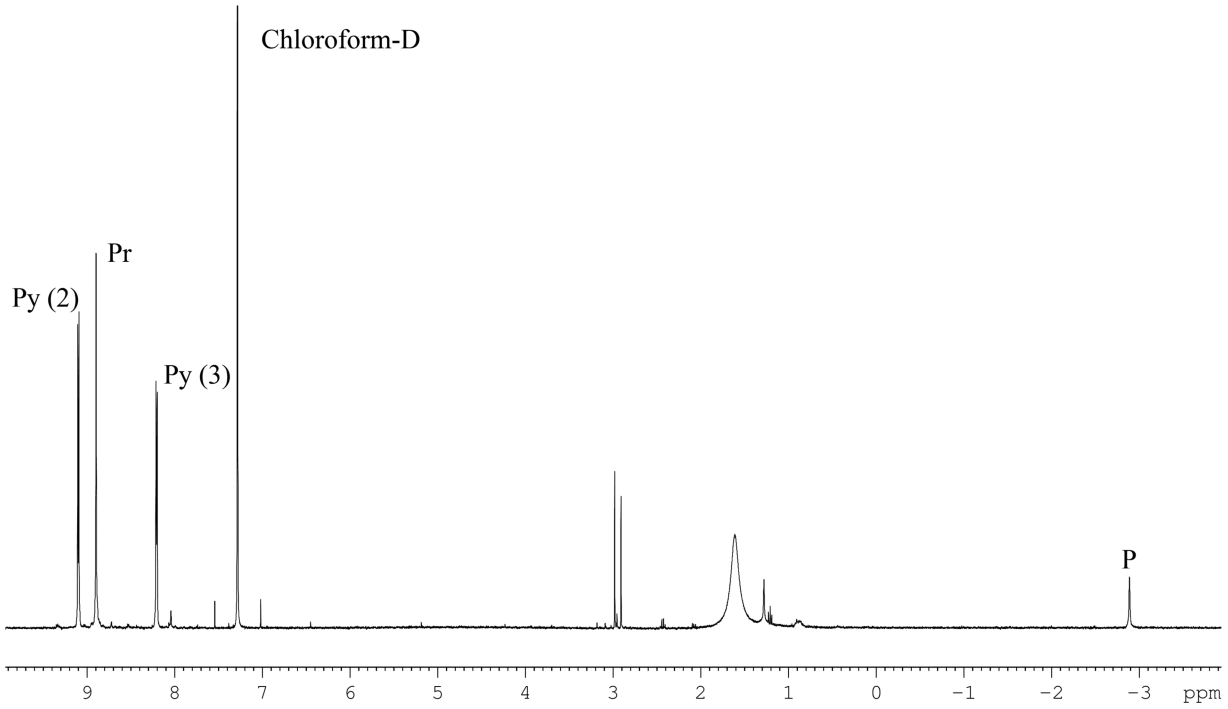

Figure 4. ^{1}H NMR spectrum of free base **TPyP** in $CDCl_3$.

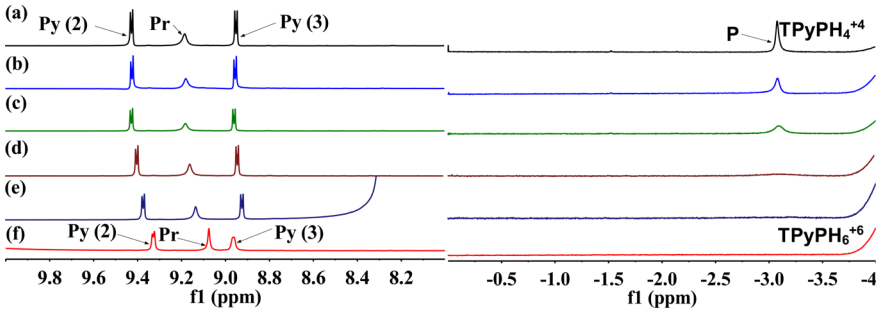

Figure 5. ^{1}H NMR spectra of **TPyP** (approximately 0.3 mM, 150 nmol) upon protonation with increasing amounts of MSA in DMSO, with the protonation state changing from $\mathbf{TPyPH_4}^{+4}$ to $\mathbf{TPyPH_6}^{+6}$ (a–f). (a) 23 μmol MSA, (b) 69 μmol MSA, (c) 177 μmol MSA, (d) 485 μmol MSA, (e) 640 μmol MSA, and (f) 1.72 mmol MSA.

NMR spectrum (Figure 5a), in which only the four peripheral pyridyl groups are protonated. Comparing the spectra between **TPyP** and $\mathbf{TPyPH_4}^{+4}$, the protonation of the peripheral pyridyl groups moves all the pyridyl proton signals and the β pyrrole proton (H_β) signal downfield. Pyridinium is expected to be a strongly electron-withdrawing group by both inductive and resonance effects, leading to deshielding of the protons on the pyridyl groups as well as the pyrrole β positions of the porphyrin. With continued acidification, protonation occurs on the internal nitrogens, leading to $\mathbf{TPyPH_6}^{+6}$, characterized by broadening and decreasing of the porphyrin N–H signals and further downfield shift of the pyridyl protons on the 2 positions. Structurally, protonation of the inner nitrogens of a porphyrin typically distorts the macrocycle from planar to nonplanar.[15] Consequently the proton exchanges of the inner ring with the solution are easier and faster, which leads to the disappearance of the porphyrin N–H signals. The intermediate stages of the titration, in which both $\mathbf{TPyPH_4}^{+4}$ and $\mathbf{TPyPH_6}^{+6}$ coexist, show only single averaged peaks, indicating that exchange between the two states is fast.

TAPP. Acid titrations of **TAPP** go through two stages. In the first stage (Figure 6), the UV–vis spectra show that the Soret band at 439 nm splits into two bands at 390 and 467 nm, the Q bands disappear, and a huge absorbance at 808 nm grows in, all characteristic of protonating the interior porphyrin nitrogens, which produces the hyperporphyrin effect.[2,9,12] In the NMR spectra during this stage ($\mathbf{TAPP} \rightarrow \mathbf{TAPPH_2}^{+2}$), substantial changes can be observed on the aminophenyl protons, which move downfield by 0.25–0.49 ppm. Meanwhile, the pyrrole H_β moves upfield by 0.59 ppm, while the internal N–H moves downfield by 3.5 ppm, indicating reduced ring current effects from the porphyrin ring. The movement of the amino NH_2 signal is also notable; upon acid titration, the original signal at 5.56 ppm is gradually replaced by a new one at 6.41 ppm. Via the hyperporphyrin resonance forms, all amino groups can bear a partial positive charge. Both the spectra of the free base and the diprotonated hyperporphyrin coexist during this stage of the titration, indicating that proton exchange is a slow process.

In the second stage of the titration (Figure 7), protons attack the aminophenyl groups and destroy the hyperporphyrin effect, resulting in the fully protonated porphyrin ($\mathbf{TAPPH_6}^{+6}$). The

DOI: 10.1021/acs.joc.5b00690
J. Org. Chem. 2015, 80, 7351–7359

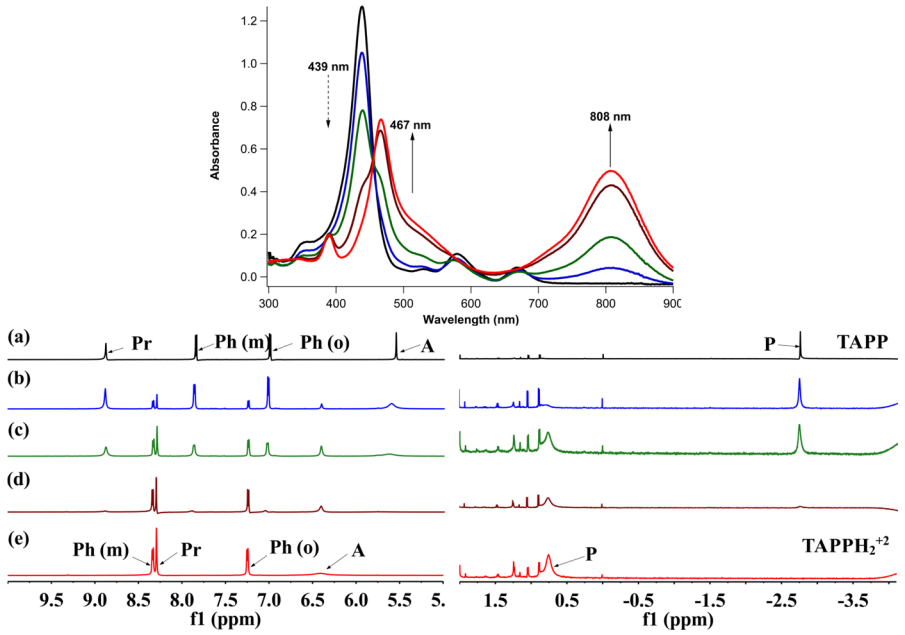

Figure 6. UV−vis and ^{1}H NMR spectra of **TAPP** (approximately 0.2 mM, 100 nmol) upon protonation from **TAPP** to **TAPPH$_2^{+2}$** (color coordinated between spectra): (a) 0 nmol MSA, (b) 300 nmol MSA, (c) 600 nmol MSA, (d) 1.1 μmol MSA, and (e) 1.5 μmol MSA.

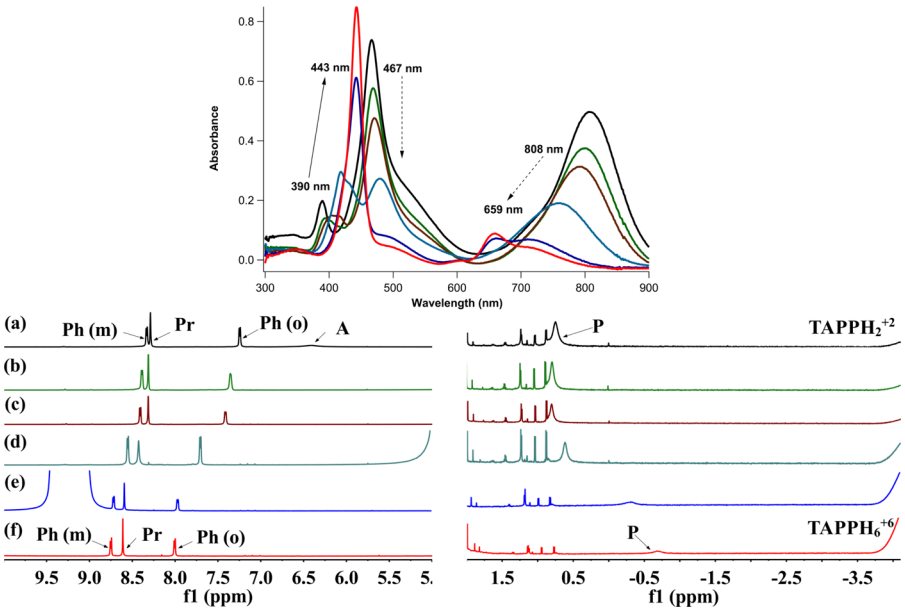

Figure 7. UV−vis and ^{1}H NMR spectra of **TAPP** (approximately 0.2 mM, 100 nmol) upon protonation from **TAPPH$_2^{+2}$** to **TAPPH$_6^{+6}$** (color coordinated between spectra): (a) 1.5 μmol MSA, (b) 9.2 μmol MSA, (c) 15 μmol MSA, (d) 92 μmol MSA, (e) 630 μmol MSA, and (f) 1.25 mmol MSA.

spectroscopy is characterized by growth of a sharp new Soret band at 443 nm and disappearance of the strong hyperporphyrin band at 808 nm in favor of a single Q-band at 659 nm. In the NMR spectra, all the aromatic protons and the pyrrole H$_\beta$ move downfield by 0.41−0.76 ppm, along with the disappearance of the amino NH$_2$. The internal N−H signal moves upfield to −0.7 ppm and broadens. In this stage of the titration, the peaks shift gradually, indicating rapid exchange between the species in equilibrium.

A$_3$PyP. Both the UV−vis spectroscopy and the NMR spectral changes of **A$_3$PyP** are comparable to those of **TAPP**. The spectrum is substantially more complex, however, because of the presence of one pyridyl and three aminophenyl groups (two cis and one trans to the pyridyl group). Initial protonation occurs on the interior porphyrin nitrogens and induces the hyperporphyrin effect; the peripheral pyridyl group is also protonated, forming **A$_3$PyPH$_3^{+3}$** (Figure 8).

In the UV−vis spectrum of **A$_3$PyPH$_3^{+3}$**, a strong hyperporphyrin absorption appears at 788 nm as well as a split Soret band characteristic of a hyperporphyrin. In the NMR spectrum, the phenyl signals appear in two absorptions with an intensity ratio close to 2:1; two of the aminophenyl groups are cis to the pyridinium substituent, and one is trans. The distinction is subtle in the neutral form but very clear in the hyperporphyrin. The presence of two amino −NH$_2$ peaks can be explained in the same way. The internal N−H signals also move downfield and appear

DOI: 10.1021/acs.joc.5b00690
J. Org. Chem. 2015, 80, 7351−7359

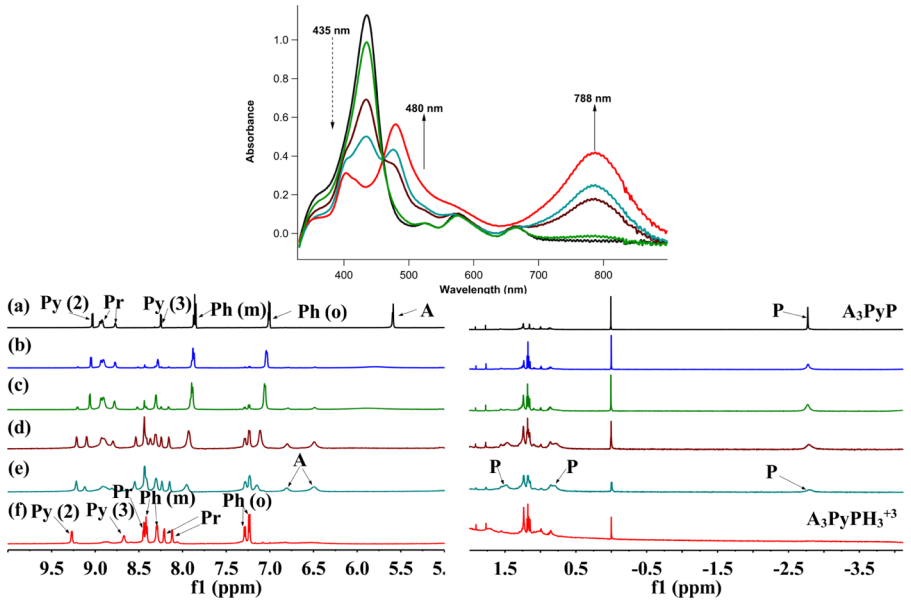

Figure 8. UV−vis and ^{1}H NMR spectra of $\mathbf{A_3PyP}$ (approximately 0.4 mM, 200 nmol) upon protonation from $\mathbf{A_3PyP}$ to $\mathbf{A_3PyPH_3}^{+3}$ (color coordinated between spectra): (a) 0 mmol MSA, (b) 46 nmol MSA, (c) 150 nmol MSA, (d) 460 nmol MSA, (e) 620 nmol MSA, and (f) 1.23 μmol MSA.

as two signals of comparable intensity, especially notable in the spectrum of Figure 8e. In all cases, the NMR absorptions of both the neutral porphyrin and the hyperporphyrin appear together, indicating slow exchange between the species.

The final stage of titration to $\mathbf{A_3PyPH_6}^{+6}$ (Figure 9) features the formation of a single Soret band (at 447 nm) and a single Q-band (at 659 nm) as the strong hyperporphyrin band at 788 nm disappears, similar to what is observed for **TAPP**. In the NMR spectra, this process is characterized by the downfield shift of all the proton signals, consistent with increased aromaticity as well as increased positive charge. The interior NH protons of the porphyrin are not detectable, presumably rapidly exchanging. The NMR signals shift gradually, indicating that the species present are in rapid equilibrium.

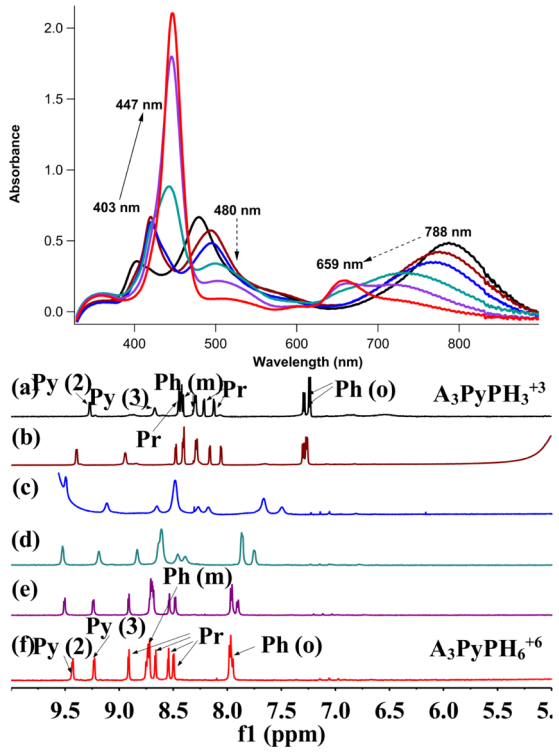

Figure 9. UV−vis and ^{1}H NMR spectra of $\mathbf{A_3PyP}$ (approximately 0.4 mM, 200 nmol) upon protonation from $\mathbf{A_3PyPH_3}^{+3}$ to $\mathbf{A_3PyPH_6}^{+6}$ (color coordinated between spectra): (a) 1.23 μmol MSA, (b) 23 μmol MSA, (c) 250 μmol MSA, (d) 480 μmol MSA, (e) 940 μmol MSA, and (f) 1.7 mmol MSA.

Comparison of NMR Spectra at Different States. Additional UV−vis and NMR spectra for $\mathbf{APy_3P}$ and $\mathbf{cis\text{-}A_2Py_2P}$ are presented in the Supporting Information (Figures S1−S4) in the same format as Figures 6−9. Table 1 summarizes the NMR features of each of the aminophenyl/pyridyl porphyrins in each state: free base, partially protonated (some of which are hyperporphyrins), and fully protonated.

2D NMR Spectra of $\mathbf{A_3PyP}$ States. In order to gain further insight into the structural details of the hyperporphyrin $\mathbf{A_3PyPH_3}^{+3}$ as well as accurately assign each proton signal to individual hydrogens, COSY and NOESY (hydrogen−hydrogen) spectra of $\mathbf{A_3PyP}$ in various protonation states were studied. As shown in the NOESY for free base $\mathbf{A_3PyP}$ (Figure 10), the phenyl protons at 7.0 ppm interact with both the amino group at 5.6 ppm as well as the neighboring phenyl protons at 7.8 ppm; these are assigned to the hydrogens at the ortho positions. The hydrogens on the pyridyl-2 (9.1 ppm) and pyridyl-3 (8.3 ppm) positions also clearly interact with one another. Small interactions between the pyrrole hydrogens (8.8 and 8.9 ppm) are also detectable. Significantly, there is a small interaction detected between the hydrogen at the phenyl meta position (7.8 ppm) and one of the pyrrole hydrogens (at 8.9 ppm). This interaction is at a significant distance through space, and it was further examined by comparing the COSY and NOESY spectra of the hyperporphyrin (Figure 11).

In both the COSY and NOESY spectra of the hyperporphyrin $\mathbf{A_3PyPH_3}^{+3}$, the ortho phenyl hydrogens at 7.23 and 7.29 ppm interact strongly with the meta phenyl hydrogens at 8.29 and 8.42 ppm; in the hyperporphyrin the aminophenyls are clearly split into two groups in a 2:1 intensity ratio, corresponding to the aminophenyls that are either cis or trans to the pyridyl group,

DOI: 10.1021/acs.joc.5b00690
J. Org. Chem. 2015, 80, 7351−7359

Table 1. Proton Chemical Shifts (ppm) of the Various Hydrogens of Aminophenyl/Pyridyl Porphyrins in Each Protonation State

compound	phenyl (o/m)	pyrrole (β)	amino (NH_2)	porphyrin (NH)	pyridine (3/2)
		Free Base			
TPyP	–	9.06	–	−2.93	8.16/9.07
APy_3P	7.02/7.87	8.87/9.03	5.65	−2.93	8.26/9.05
cis-A_2Py_2P	7.01/7.87	8.8/8.83/8.96/8.98	5.62	−2.83	8.25/9.03
A_3PyP	7.00/7.86	8.77/8.92/8.94	5.59	−2.77	8.24/9.03
TAPP	7.00/7.85	8.88	5.56	−2.74	–
		Partially Protonated			
$TPyPH_4^{+4}$	–	9.18	–	–	8.92/9.41
$APy_3PH_5^{+5}$	7.84/8.39	9.09/9.15	–	–	8.99/9.41
cis-$A_2Py_2PH_4^{+4}$	7.69/8.27	---	–	–	8.87/9.38
$A_3PyPH_3^{+3}$	7.23/8.29 7.29/8.42	8.12/8.21/8.44	–	–	8.67/9.27
$TAPPH_2^{+2}$	7.25/8.34	8.29	6.41	0.76	–
		Fully Protonated			
$TPyPH_6^{+6}$	–	9.08	–	–	8.96/9.32
$APy_3PH_6^{+6}$	7.91/8.58	8.72/8.86/8.99	–	–	9.22/9.35
cis-$A_2Py_2PH_6^{+6}$	7.92/8.72	8.46/8.62/8.83/9.00	–	–	9.22/9.42
$A_3PyPH_6^{+6}$	7.97/8.73	8.50/8.54/8.66/8.91	–	–	9.23/9.43
$TAPPH_6^{+6}$	8.01/8.75	8.61	–	−0.70	–

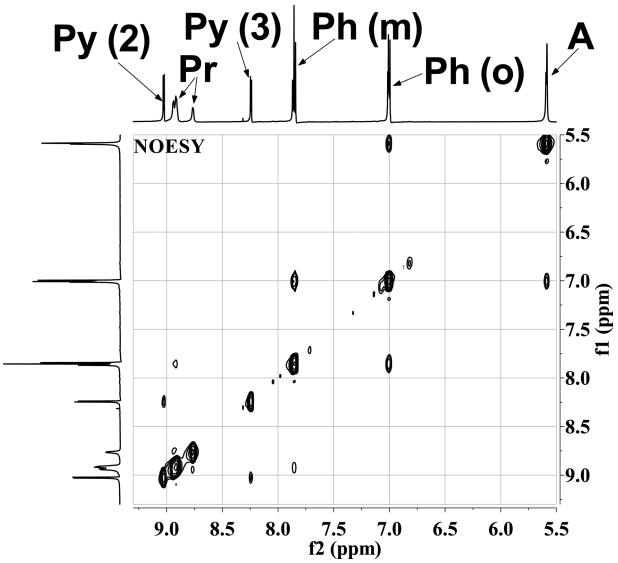

Figure 10. NOESY of free base **A_3PyP**.

respectively. One of the meta peaks overlaps with a pyrrole peak, but they can be distinguished via the interaction with the ortho hydrogens. The strength of the ortho/meta interactions is considered a standard benchmark to use as a measure of the importance of different interactions. The interaction between pyridyl 2 and 3 hydrogens at 9.27 and 8.67 ppm is still present, but weaker in the COSY and more intense in the NOESY. The COSY shows no other significant interactions. The NOESY, on the other hand, shows all of these as well as several additional interactions. Most notably, a broad peak at about 8.8 ppm shows interactions with phenyl meta hydrogens and pyrrole hydrogens. This broad peak can be traced to small amounts of unprotonated **A_3PyP** still present (see the UV−vis spectra of Figure 8) and chemical exchange with the primary species present, **$A_3PyPH_3^{+3}$**, by rapid proton exchange.

Figure 11 highlights in red two interactions in which pyrrole hydrogens interact through space with nearby hydrogens on the aminophenyl meta position and the pyridyl 3 position. The meta phenyl hydrogens interact with a pyrrole β hydrogen at 8.21 ppm, and the hydrogens on the 3 position of the pyridyl group (at 8.67 ppm) interact with a different pyrrole β hydrogen (at 8.45 ppm). Taken together, these data suggest that the porphyrin has become more coplanar with the aminophenyl and pyridyl substituents, such that these meso substituents have moved closer to the pyrrole β hydrogens. This is consistent with the strong resonance effects between the substituents and the porphyrin core proposed in the hyperporphyrin structure and as observed in the UV−vis spectra.

When the porphyrin is fully protonated (Figure 12), the COSY shows only the interactions between hydrogens bonded on the same units, i.e., phenyl ortho/meta, pyridyl 2/3, and pyrrole β hydrogens. The NOESY shows all of these but also continues to show weak interactions between meta hydrogens on the aminophenyl groups (8.73 ppm) with pyrrole β hydrogens (8.50 and 8.54 ppm) as well as interactions of 3 hydrogens on the pyridyl groups (9.23 ppm) with the pyrrole β hydrogens (8.91 ppm). Insofar as these interactions appear weaker than they are in the hyperporphyrin spectra, these data suggest that the substituents have rotated farther out of the plane of the porphyrin, as expected for fully protonated substituents without resonance interactions to contribute to the porphyrin core.

■ DISCUSSION

NMR spectroscopy of the protonated forms of variously substituted *p*-(dimethylamino)phenylporphyrins has been reported.[11,16] The effects seen there for the tetra-substituted case completely parallel those seen here for **TAPP**. In those studies, the alternative substituents were unsubstituted phenyl groups, so that the effects of only the strongly electron-donating dimethylamino groups were under consideration. In this study, we have added strongly electron-withdrawing pyridinium substituents to determine potential push−pull effects on hyperporphyrin spectroscopy and structure. In the series of aminophenyl/pyridyl porphyrins studied here, the sequence in which the aminophenyl, pyridyl, and pyrrole nitrogens are protonated plays an important role in tracking the UV−vis and NMR spectra. In **TPyP** and **APy_3P**, the basicities of the pyridyl groups are stronger than those of the pyrrole nitrogens, so pyridyl groups are converted to pyridinium first.[12] However, with two or more aminophenyl groups, the basicities of the pyrrole

DOI: 10.1021/acs.joc.5b00690
J. Org. Chem. 2015, 80, 7351−7359

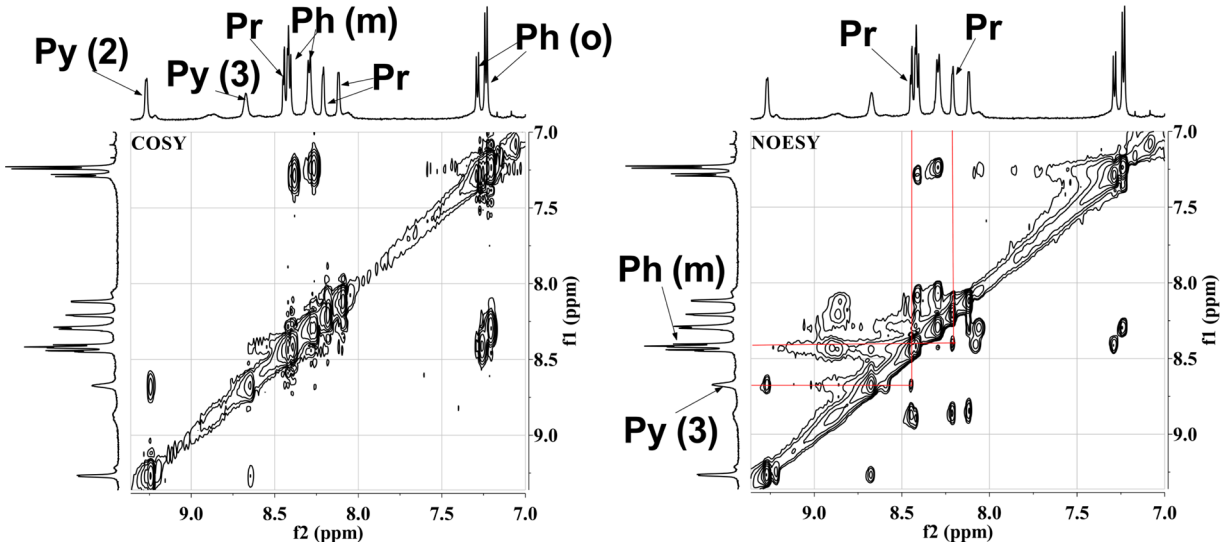

Figure 11. COSY and NOESY of hyperporphyrin $\mathbf{A_3PyPH_3}^{+3}$.

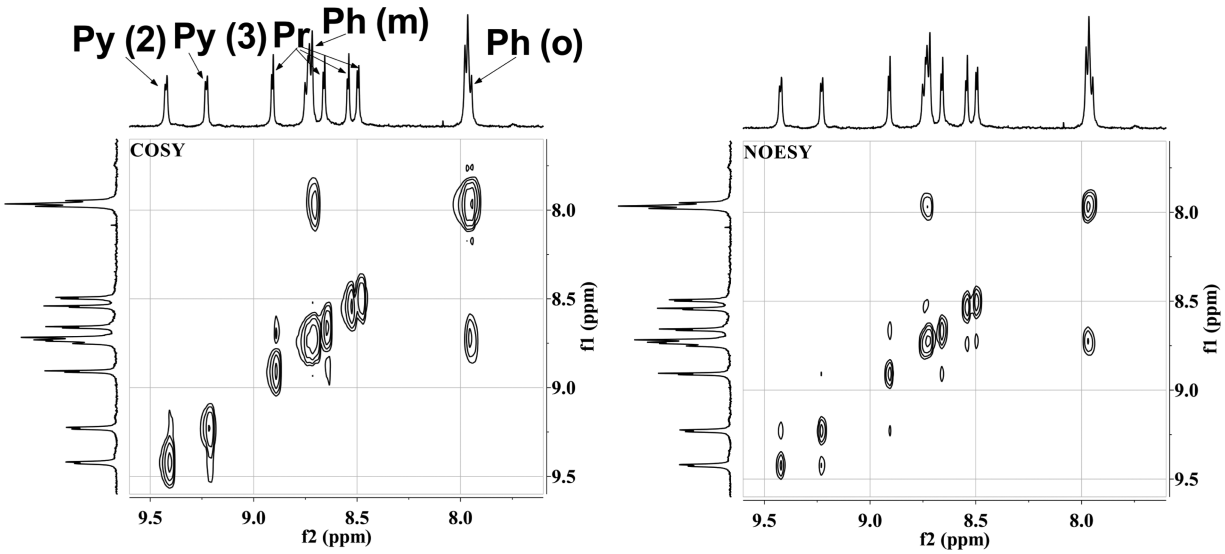

Figure 12. COSY and NOESY of fully protonated $\mathbf{A_3PyPH_6}^{+6}$.

nitrogens are enhanced, so that for **cis-A_2Py_2P** and **A_3PyP**, the protonations of pyridyl groups and pyrrole nitrogens are observed at the same time. It has been suggested that for **A_3PyP** the protonation of pyrrole nitrogens may occur prior to protonation of pyridyl group, but the spectroscopic changes are too subtle to clearly distinguish this possibility;[12] we found no evidence in the NMR spectra to support this possibility either.

The proton NMR spectra of porphyrins have been determined to be dominated by the large π-electron ring current of the macrocycle and inductive effects of the peripheral groups.[17] The hyperporphyrin effect requires significant coplanarity of the meso aromatic groups with the porphyrin macrocycle to facilitate resonance charge-transfer effects. In order to accommodate the coplanarity, adjacent pyrroles tilt, which results in distortion of the macrocycle. The ring current decreases in consequence, with characteristic movements upfield for the pyrrole H_β and downfield for the internal N−H protons.[18] Although they all show a hyperporphyrin effect, the NMR spectra of **APy_3P**, **cis-A_2Py_2P**, **A_3PyP**, and **TAPP** under acidification are quite different. **$TAPPH_2^{+2}$** and **$A_3PyPH_3^{+3}$** exhibit strong hyperporphyrin effects in their UV−visible spectra; they also show the upfield shift of H_β characteristic of the ring distortion caused by a hyperporphyrin. In comparison, **$APy_3PH_5^{+5}$** and **cis-$A_2Py_2PH_4^{+4}$** show a shift of H_β downfield instead. It is notable that the spectroscopic signatures of the hyperporphyrins from **$APy_3PH_5^{+5}$** and **cis-$A_2Py_2PH_4^{+4}$** are quite weak. In these cases, the strong electron-withdrawing effect of the multiple pyridinium groups appears to exert a larger effect than a relatively small ring distortion.[19]

Evidence in the 1D and 2D proton NMR spectra of **$A_3PyPH_3^{+3}$** support the idea that a type D resonance form (see Figure 1) is a significant contributor to the hyperporphyrin structure. The coexistence of the individual spectra of both the free base and hyperporphyrin indicates slow exchange between the two states, suggesting a significant change of geometry. Increased distortion of the porphyrin macrocycle to accommodate resonance interactions with the meso substituents is indicated by the decreased effects of ring current on chemical shifts of the pyrrole β hydrogens and the internal NH of the porphyrin. The 2D NOESY indicates that nearby hydrogens on

DOI: 10.1021/acs.joc.5b00690
J. Org. Chem. 2015, 80, 7351−7359

the porphyrin macrocycle and the meso substituents interact more strongly, specifically pyrrole β hydrogens with the pyridyl-3 and phenyl meta hydrogens. The aminophenyl groups of $\mathbf{A_3PyPH_3}^{+3}$ appear as two separate signals in approximately a 2:1 intensity ratio, due to the cis and trans orientations of the aminophenyl groups to the pyridyl group. This distinction should also be present, but is barely detectable, in the neutral or fully protonated form, where it is quite distinct in the hyperporphyrin spectrum. In the hyperporphyrin, the two cis aminophenyl groups can interact with either the pyridinium (type D) or the neighboring aminophenyl (type C), but the trans aminophenyl can only participate in type C interactions.

Examination of chemical shifts provides additional evidence for the importance of the type D resonance form in the hyperporphyrin structure (Table 1, with selected data abstracted into Table 2). The chemical shifts for protons on neutral pyridyl groups in free base porphyrins are all comparable, e.g., **TPyP** (8.16/9.07) and $\mathbf{A_3PyP}$ (8.24/9.03). Similarly, the C−H protons on protonated pyridinium groups are also comparable for all porphyrins, e.g., $\mathbf{TPyPH_4}^{+4}$ (8.92/9.41) and $\mathbf{TPyPH_6}^{+6}$ (8.96/9.32). In contrast, the pyridinium group in the hyperporphyrin $\mathbf{A_3PyPH_3}^{+3}$ shows chemical shifts of 8.67 and 9.27 ppm, intermediate between a neutral and a positive pyridyl group. Similar effects are seen with the chemical shifts of the phenyl C−H absorptions. Where neutral aminophenyls have chemical shifts of 7.00 and 7.85 ppm and fully protonated aminophenyl groups have chemical shifts of 8.01 and 8.75 ppm, the hyperporphyrin $\mathbf{TAPPH_2}^{+2}$ shows chemical shifts of 7.25 and 8.34 ppm, intermediate between a neutral and a positive aminophenyl. The two different aminophenyls in the $\mathbf{A_3PyPH_3}^{+3}$ hyperporphyrin show chemical shifts of 7.23/7.29 and 8.29/8.42 ppm. Thus, the NMR data suggest a structure for aminophenyl groups in hyperporphyrins having partial positive charge; the chemical shifts fall between those of neutral aminophenyl and fully protonated aminophenyl by about 25% for meta and 50% for ortho, consistent with expectations for resonance delocalization. Similarly, the chemical shifts for the pyridyl protons in $\mathbf{A_3PyPH_3}^{+3}$ fall between those of neutral and protonated pyridyl groups by about 50−60%, comparable for both the 2 and 3 positions.

Table 2. Aminophenyl and Pyridyl Proton Chemical Shifts in Hyperporphyrins Compared to Standards from TPyP and TAPP

	Aminophenyl (o / m)		Pyridyl (3 / 2)
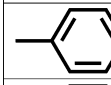	7.00/7.85 (**TAPP**)	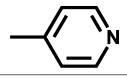	8.16/9.07 (**TPyP**)
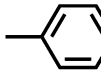	8.01/8.75 ($\mathbf{TAPPH_6}^{+6}$)	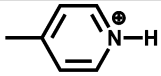	8.92/9.41 ($\mathbf{TPyPH_4}^{+4}$) 8.96/9.32 ($\mathbf{TPyPH_6}^{+6}$)
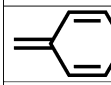		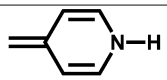	
$\mathbf{TAPPH_2}^{+2}$	7.25/8.34		
$\mathbf{A_3PyPH_3}^{+3}$	7.23/8.29 7.29/8.42	$\mathbf{A_3PyPH_3}^{+3}$	8.67/9.27

EXPERIMENTAL SECTION

Materials. Solvents and reagents were the highest grade commercially available and used as received.

Preparation of Carbomethoxy/Pyridylporphyrins ($\mathbf{CM_xPy_yP}$). 4-Carbomethoxybenzaldehyde (1.64 g, 11.1 mmol) and 4-pyridinecarboxaldehyde (3.30 g, 30.8 mmol) were dissolved in 62.5 mL propionic acid. The solution was heated to reflux, and pyrrole (2.80 g, 41.8 mmol) was slowly added. After heating for 1 h and cooling to room temperature, the majority of the propionic acid was removed by vacuum distillation at 150 °C. The remaining solution was neutralized using aqueous NaOH, and the porphyrin was extracted with chloroform.

Column chromatography (silica gel 230−400 mesh) eluting with $CHCl_3$ and ethyl acetate (20%−100%) and 1% triethylamine yielded $\mathbf{CM_3PyP}$, $\mathbf{CM_2Py_2P}$ (cis), and $\mathbf{CMPy_3P}$ (where CM represents the 4-carbomethoxyphenyl substituents).

5,10,15-Tris(4-carbomethoxyphenyl)-20-(4-pyridyl)porphyrin ($\mathbf{CM_3PyP}$). 0.3378 g $\mathbf{CM_3PyP}$ (2% of the theoretical yield) was eluted with (4:1) CH_2Cl_2:ethyl acetate (0.1% Et_3N) from a silica column. ^{1}H NMR (400 MHz, $CDCl_3$) δ 9.05 (d, J = 5.9 Hz, 2H), 8.89−8.77 (m, 8H), 8.45 (d, J = 8.3 Hz, 6H), 8.29 (d, J = 8.2 Hz, 6H), 8.16 (d, J = 5.9 Hz, 2H), 4.12 (s, 9H), −2.84 (s, 2H). ^{13}C NMR (101 MHz, $CDCl_3$) δ 167.2, 150.1, 148.4, 146.5, 134.5, 129.9, 129.4, 128.0, 119.8, 119.6, 117.1, 52.5. HRMS (ESI/LTQ-Orbitrap) m/z: $[M + H]^+$ calcd for $C_{49}H_{36}N_5O_6$, 790.2660; found, 790.2676.

5,10-Bis(4-carbomethoxyphenyl)-15,20-bis(4-pyridyl)porphyrin (cis-$\mathbf{CM_2Py_2P}$). 0.0534 g cis-$\mathbf{CM_2Py_2P}$ (0.3% of the theoretical yield) was eluted with (4:1) CH_2Cl_2:ethyl acetate (0.1% Et_3N) from a silica column. ^{1}H NMR (400 MHz, $CDCl_3$) δ 9.06 (d, J = 5.9 Hz, 4H), 8.85 (d, J = 8.7 Hz, 8H), 8.46 (d, J = 8.3 Hz, 4H), 8.30 (d, J = 8.4 Hz, 4H), 8.16 (d, J = 5.9 Hz, 4H), 4.12 (s, 6H), −2.86 (s, 2H). ^{13}C NMR (101 MHz, $CDCl_3$) δ 167.2, 150.0, 148.4, 146.4, 134.5, 130.0, 129.4, 128.1, 120.0, 117.3, 52.5. HRMS (ESI/LTQ-Orbitrap) m/z: $[M + H]^+$ calcd for $C_{46}H_{33}N_6O_4$, 733.2558; found, 733.2572.

5-(4-Carbomethoxyphenyl)-10,15,20-tris(4-pyridyl)porphyrin ($\mathbf{CMPy_3P}$). 0.0235 g $\mathbf{CMPy_3P}$ (0.1% of the theoretical yield) was eluted with (4:1) CH_2Cl_2:ethyl acetate (0.1% Et_3N) from a silica column. ^{1}H NMR (400 MHz, $CDCl_3$) δ 9.06 (d, J = 5.9 Hz, 6H), 8.92−8.79 (m, 8H), 8.47 (d, J = 8.3 Hz, 2H), 8.30 (d, J = 8.4 Hz, 2H), 8.16 (d, J = 5.9 Hz, 6H), 4.12 (s, 3H), −2.89 (s, 2H). ^{13}C NMR (101 MHz, $CDCl_3$) δ 167.2, 149.9, 148.4, 146.3, 134.5, 130.0, 129.4, 128.1, 117.7, 117.5, 52.5. HRMS (ESI/LTQ-Orbitrap) m/z: $[M + H]^+$ calcd for $C_{43}H_{30}N_7O_2$, 676.2456; found, 676.2471.

Preparation of $\mathbf{A_xPy_yP}$. A Lossen rearrangement was run on each of these individually isolated porphyrins to prepare the corresponding aminophenyl/pyridyl porphyrins ($\mathbf{A_xPy_yP}$).[20] Each individual $\mathbf{CM_xPy_yP}$ derivative and 8 equiv $NH_2OH{\cdot}HCl$ were warmed to 100 °C in polyphosphoric acid, and the solution was slowly heated to 160 °C over 3 h. Upon cooling to room temperature, aqueous NaOH was slowly added to neutralize the solution, and the porphyrin was extracted with chloroform. Column chromatography was then used to remove any residual starting material by eluting with $CHCl_3$ and MeOH (5%).

5,10,15-Tris(4-aminophenyl)-20-(4-pyridyl)porphyrin ($\mathbf{A_3PyP}$). UV−vis (DMSO): λ_{max}, nm (ε*10^3) 434 (194), 525 (15), 575 (21), 664 (12). ^{1}H NMR (600 MHz, DMSO) δ 9.03 (d, J = 5.8 Hz, 2H), 8.98−8.87 (m, 6H), 8.77 (s, 2H), 8.24 (d, J = 5.8 Hz, 2H), 7.85 (d, J = 8.2 Hz, 6H), 7.00 (d, J = 8.3 Hz, 6H), 5.59 (s, 6H), −2.77 (s, 2H). ^{13}C NMR (101 MHz, $CDCl_3$) δ 148.2 (s), 146.1 (s), 135.7 (s), 132.3 (s), 129.6 (s), 120.7 (s), 113.5 (s). HRMS (ESI/LTQ-Orbitrap) m/z: $[M + H]^+$ calcd for $C_{43}H_{33}N_8$, 661.2823; found, 661.2824.

5,10-Bis(4-aminophenyl)-15,20-bis(4-pyridyl)porphyrin (cis-$\mathbf{A_2Py_2P}$). UV−vis (DMSO): λ_{max}, nm (ε*10^3) 419 (138), 518 (11), 571 (10), 657 (5). ^{1}H NMR (600 MHz, DMSO) δ 9.03 (d, J = 5.7 Hz, 4H), 8.97 (d, J = 15.5 Hz, 3H), 8.81 (d, J = 15.5 Hz, 4H), 8.25 (d, J = 5.8 Hz, 4H), 7.87 (d, J = 8.2 Hz, 4H), 7.01 (d, J = 8.3 Hz, 4H), 5.62 (s, 4H), −2.83 (s, 2H). ^{13}C NMR (101 MHz, $CDCl_3$) δ 150.4 (s), 148.3 (s), 146.3 (s), 135.8 (s), 129.5 (s), 116.1 (s), 113.5 (s). HRMS (ESI/LTQ-Orbitrap) m/z: $[M + H]^+$ calcd for $C_{42}H_{31}N_8$, 647.2666; found, 647.2663.

5-(4-Aminophenyl)-10,15,20-tris(4-pyridyl)porphyrin ($\mathbf{APy_3P}$). UV−vis (DMSO): λ_{max}, nm (ε*10^3) 418 (254), 515 (11), 554 (3), 589 (4), 650 (1). ^{1}H NMR (600 MHz, DMSO) δ 9.05 (d, J = 5.7 Hz, 6H), 9.02 (d, J = 3.4 Hz, 1H), 8.87 (s, 5H), 8.27 (d, J = 5.8 Hz, 6H), 7.87 (d, J = 8.2 Hz, 2H), 7.02 (d, J = 8.2 Hz, 2H), 5.65 (s, 2H), −2.93 (s, 2H).

DOI: 10.1021/acs.joc.5b00690
J. Org. Chem. 2015, 80, 7351−7359

^{13}C NMR (101 MHz, $CDCl_3$) δ 148.4 (s), 148.3 (s), 129.4 (s), 113.6 (s). HRMS (ESI/LTQ-Orbitrap) m/z: $[M + H]^+$ calcd for $C_{41}H_{29}N_8$, 633.2510; found, 633.2511.

Instruments. UV−visible spectra were run from 300 to 900 nm using a single visible light source and a single detector. Scanning speed was medium with sample interval of either 0.2 or 1 nm and a slit width of 3 nm. The UV−vis spectroscopy measurements in this study were obtained using small aliquots taken directly from the same solutions used for the NMR studies. Because the concentration of the porphyrin solutions for the NMR studies was too high to use a standard cuvette, a special thin-layer cell was prepared as follows: Standard microscopic slides were first cut into appropriate sizes (3.5 × 1.5 cm) and cleaned with Sparkleen and water then rinsed in DI water for 20 min and dried in an oven at 100°. On one slide, two layers of Parafilm were wrapped, leaving a 1 cm space. A second slide was pressed against the wrapped one and fixed in place with additional Parafilm wrapped around the outer ends. Sample solution is added by a capillary pipet, and the cell is mounted onto a customized holder for UV−vis measurements (Figure 13).

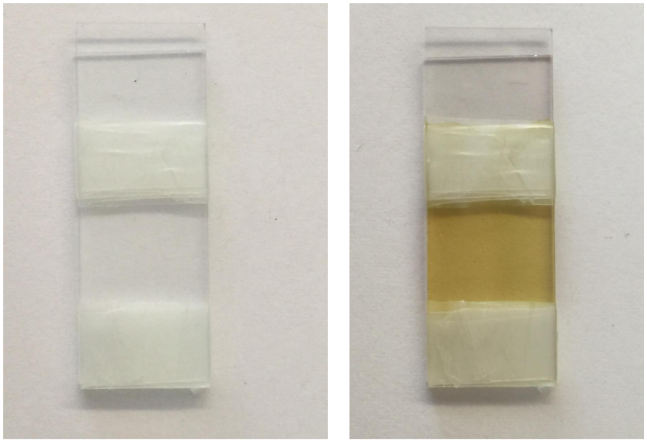

(a) (b)

Figure 13. Pictures of thin-layer cell slides (a) before adding porphyrin solution and (b) after adding concentrated porphyrin solution.

1D proton and carbon-13 data were collected at 25 °C over a scan range from −4 to 16 ppm (^{1}H) and −4 to 240 ppm (^{13}C).

Titrations. In the NMR tube, concentrated solutions of porphyrin in 500 μL of deuterated DMSO were titrated with MSA. Acid of appropriate concentration was added in 10−20 μL increments, with the sample mixed between each addition using a shaker.

■ ASSOCIATED CONTENT

Supporting Information

UV−vis and NMR spectra of the acid titrations of **cis-A_2Py_2P** and **APy_3P** are presented in the same format as Figures 6−9. Proton and C-13 NMR spectra as well as high-resolution mass spectra are presented for **A_3PyP**, **CM_3PyP**, **cis-A_2Py_2P**, **cis-CM_2Py_2P**, **APy_3P**, and **$CMPy_3P$**. The Supporting Information is available free of charge on the ACS Publications website at DOI: 10.1021/acs.joc.5b00690.

■ AUTHOR INFORMATION

Corresponding Author

*E-mail: wamserc@pdx.edu.

Notes

The authors declare no competing financial interest.

■ ACKNOWLEDGMENTS

Support from the Oregon Nanoscience and Microtechnologies Institute (ONAMI) and the National Science Foundation (Grant CHE-0911186) is gratefully acknowledged. Development of the thin-layer spectrophotometric cell was by Keith James. Helpful discussions with Professor David Peyton are gratefully acknowledged. This work partially comprised the Ph.D. Dissertation of Chenyi Wang at Portland State University (2015).

■ REFERENCES

(1) Gouterman, M. In *The Porphyrins*; Dolphin, D., Ed.; Academic Press: New York, 1978; Vol. *III*, pp 1−165.
(2) Ojadi, E. C. A.; Linschitz, H.; Gouterman, M.; Walter, R. I.; Lindsey, J. S.; Wagner, R. W.; Droupadi, P. R.; Wang, W. *J. Phys. Chem.* **1993**, *97*, 13192−7.
(3) Antipas, A.; Buchler, J. W.; Gouterman, M.; Smith, P. D. *J. Am. Chem. Soc.* **1978**, *100* (10), 3015−3024.
(4) Antipas, A.; Buchler, J. W.; Gouterman, M.; Smith, P. D. *J. Am. Chem. Soc.* **1980**, *102* (1), 198−207.
(5) Gouterman, M.; Hanson, L. K.; Khalil, G. E.; Leenstra, W. R.; Buchler, J. W. *J. Chem. Phys.* **1975**, *62* (6), 2343−2353.
(6) Gouterman, M.; Schwarz, F. P.; Smith, P. D.; Dolphin, D. *J. Chem. Phys.* **1973**, *59* (2), 676−690.
(7) Sayer, P.; Gouterman, M.; Connell, C. R. *J. Am. Chem. Soc.* **1977**, *99* (4), 1082−1087.
(8) Koleva, B. B.; Kolev, T.; Seidel, R. W.; Tsanev, T.; Mayer-Figge, H.; Spiteller, M.; Sheldrick, W. S. *Spectrochim. Acta, Part A* **2008**, *71* (2), 695−702.
(9) Rudine, A. B.; DelFatti, B. D.; Wamser, C. C. *J. Org. Chem.* **2013**, *78* (12), 6040−6049.
(10) Vitasovic, M.; Gouterman, M.; Linschitz, H. *J. Porphyrins Phthalocyanines* **2001**, *5* (3), 191−197.
(11) Walter, R. I.; Ojadi, E. C. A.; Linschitz, H. *J. Phys. Chem.* **1993**, *97* (50), 13308−13312.
(12) Wang, C.; Wamser, C. C. *J. Phys. Chem. A* **2014**, *118* (20), 3605−3615.
(13) Weinkauf, J. R.; Cooper, S. W.; Schweiger, A.; Wamser, C. C. *J. Phys. Chem. A* **2003**, *107*, 3486−3496.
(14) Barton, E. E.; Rampulla, D. M.; Bocarsly, A. B. *J. Am. Chem. Soc.* **2008**, *130* (20), 6342−6344.
(15) Stone, A.; Fleischer, E. B. *J. Am. Chem. Soc.* **1968**, *90* (11), 2735−2748.
(16) Gunter, M.; Robinson, B. *Aust. J. Chem.* **1989**, *42* (11), 1897−1905.
(17) Zakavi, S.; Omidyan, R.; Ebrahimi, L.; Heidarizadi, F. *Inorg. Chem. Commun.* **2011**, *14* (11), 1827−1832.
(18) Smith, K. M.; Bobe, F. W.; Minnetian, O. M.; Abraham, R. J. *Tetrahedron* **1984**, *40* (17), 3263−3272.
(19) Mohajer, D.; Zakavi, S.; Rayati, S.; Zahedi, M.; Safari, N.; Khavasi, H. R.; Shahbazian, S. *New J. Chem.* **2004**, *28* (12), 1600−1607.
(20) Walter, M. G.; Wamser, C. C.; Ruwitch, J.; Zhao, Y.; Braden, D.; Stevens, M.; Denman, A.; Pi, R.; Rudine, A.; Pessiki, P. J. *J. Porphyrins Phthalocyanines* **2007**, *11* (8), 601−612.

DOI: 10.1021/acs.joc.5b00690
J. Org. Chem. 2015, 80, 7351−7359